Materials Science-Poland, 42(1), 2024, pp. 158-170
http://www.materialsscience.pwr.wroc.pl/
DOI: 10.2478/msp-2024-0013

Mechanical properties and quantum mechanical simulations of natural rubber composites with cerium complexes under aging conditions

Yilin Li[1,2,3], Yonggang Liu[1,2,3], Wei Hao[1,2,3], Zhaogang Liu[1,2,3,*], Wentao Zhang[1,2,3], Yanhong Hu[1,2,3], Jinxiu Wu[1,2,3]

[1]Inner Mongolia University of Science and Technology, Rare Earth Engineering Technology Institute, Baotou 014010
[2]Ministry of Education Key Laboratory for Green Extraction and Efficient Use of Light Rare Earth Resources, Baotou 014010
[3]Baotou Key Laboratory for Rare Earth Hydrometallurgy and Light Rare Earth Applications, Inner Mongolia Autonomous Region, Baotou 014010

Enhancing the service life of natural rubber (NR) products, including antioxidants, is crucial to prevent rubber degradation and enhance its oxidation resistance. Phenolic antioxidant 2246 and cerium complex of p-amino salicylic acid (PAS-Ce) are utilized as NR antioxidants. Numerous studies have qualitatively analyzed the antioxidant mechanisms of these compounds. Building upon this perspective, this study quantitatively assessed the protective mechanisms of these antioxidants by combining experimental data with molecular simulations. Additionally, it compared their impacts on the thermal oxidative aging performance of NR. The findings revealed that the PAS-Ce/NR system exhibited the highest mechanical performance retention following multiple days of thermal-oxidative aging. Analyzing the PAS-Ce/NR system through ATR-FTIR and DTA techniques demonstrated that it had the lowest C=O content after thermal-oxidative aging. Furthermore, calculating the activation energy required for thermal-oxidative aging decomposition using the Kissinger and FWO methods indicated that PAS-Ce/NR had the highest activation energy, suggesting superior inhibitory effects against thermal-oxidative aging. Quantum mechanical simulations also illustrated that the dissociation energy of the O-H bond in antioxidants 2246 and PAS-Ce was lower than that of the C-H bond in NR. However, PAS-Ce exhibited a quicker capture of radical species, effectively delaying the oxidation reaction rate of NR molecular chains and thus more efficiently inhibiting the aging process. These insights contribute significantly to comprehending the antioxidative mechanisms in NR aging.

Keywords: *rare earth, natural rubber, anti-aging agents, quantum mechanical simulations*

1. Introduction

Natural rubber (NR) materials were used in a wide range of industrial, scientific, and military applications due to their uniquely high elasticity and excellent overall properties. However, under the influence of other environmental factors such as temperature, oxygen, mechanical external forces, and light, rubber was susceptible to aging, resulting in a deterioration of its properties [1]. It was therefore important to study the process and mechanism of rubber aging and to take appropriate measures to improve the material's resistance to it. Among them, the addition of antioxidants was one of the most convenient and effective ways to prevent or delay the aging of NR [2]. Hindered phenolic antioxidant 2246, which was low in terms of toxicity and was environmentally friendly and highly compatible was widely used in industrial production.

Recent studies have found that rare earth elements have excellent antioxidant properties. The coordination reaction to their compounds and organic ligands containing O, S, and N atoms can prepare rare earth antioxidants with high antioxidant properties [3]. Xie et al. [4]. prepared a compound of rare-earth dysprosium (III) and the antioxidant 2-mercaptobenzimidazole (MB), which was shown to have superior thermal-oxidative aging properties than both

* E-mail: Liuzg65@163.com

© Yilin Li et al. 2024. This is an open access article distributed under the Creative Commons Attribution-NonCommercial-NoDerivatives 4.0 License. (http://creativecommons.org/licenses/by-nc-nd/4.0/)

the antioxidant MB and N-isopropyl N'-phenyl-p-phenylenediamine (IPPD) through thermal-oxidative aging studies on NR. Fang [5] et al. conducted a study on curium stearate ($LaSt_3$) The study of rare earth antioxidants showed that although $LaSt_3$ had a protective effect against thermal oxygen aging of polyvinyl chloride (PVC) at high temperatures, its protective effect at the initial stage was not obvious and it was an antioxidant suitable for long-term aging. $LaSt_3$ was then improved by combining it with a metal salt antioxidant such as Ca/Zn, which had a significant short-term protective effect, to greatly improve the protective effect of the antioxidant while reducing costs. This method also guided the study of low-cost and efficient antioxidant systems.

Zhang Yongpeng [6] et al. prepared rare earth (lanthanum, cerium, praseodymium, neodymium, samarium, and europium) type hindered phenolic antioxidants using hindered phenols as organic ligands to investigate the effects of rare earth-type hindered phenolic antioxidants on the vulcanization properties, physical properties and anti-aging properties of NR. The results showed that the NR rubber with each rare earth type hindered phenolic antioxidant had similar vulcanization properties and improved the oxidation resistance of NR vulcanized rubber, among which the rare earth lanthanum type hindered phenolic antioxidant had the best effect. Chen Zhong Bao [7] et al. prepared a new rare-earth rubber antioxidant by the complex decomposition method. The protective properties of the rare earth antioxidant on NR vulcanized rubber were investigated by mechanical property testing, infrared spectroscopy, and thermogravimetric analysis. The results showed that the antioxidant had a significant anti-aging effect on NR vulcanized rubber, and its anti-aging effect was better than that of commercially available phenolic BHT antioxidants and comparable to that of amine 4010NA antioxidants, and there was no color contamination to the rubber.

In this paper, the effects of hindered phenolic antioxidant 2246 and cerium rare-earth antioxidant on the thermal oxygen aging properties of NR were studied by combining experiments with quantum mechanical simulation, and the protective mechanism of the two antioxidants was analyzed.

2. Experimental segment

2.1. Experimental materials and instruments

NR was purchased from Shanghai Fuyou International Trade Co., Ltd, Antioxidant 2246, zinc oxide, stearic acid, sulfur, accelerator M, and accelerator DM were all analytically pure and obtained from Shanghai Aladdin Biochemical Technology Co., Ltd, and Cerium p-amino salicylate was prepared by Inner Mongolia University of Science and Technology (China).

The used instruments were the High-Temperature Thermal Ageing Test Chamber (HLH-408, Shanghai Hong Yue Test Equipment Co.); Fourier transform infrared spectroscopy (frontier, PerkinElmer USA Ltd.); Synchronous Thermal Analyzer (TGA/DSC 3+, Metteller-Toledo International Trading Ltd); Mixer (KY-3220, Qingdao Xincheng Yiming Acorn Plastic Machinery Co. Ltd.); Opener (160, Hou Street, Dongguan City); Universal Test Machine (AL-7000 MU2A, High-Speed Rail Testing Instrument (Dongguan) Co. Ltd); Universal Prototyping Machine (WZY-15, High-Speed Rail Testing Instrument (Dongguan) Co. Ltd); and Shao hardness meter (LX-4, Dongguan Gaoxin Testing Equipment Co. Ltd).

2.2. Preparation of samples

The NR formula is shown in Table 1.

Preparation of PAS-Ce/NR, 2246/NR, and NR samples were prepared according to the following procedure: First, NR compounds were mixed in a two-roll mill (Dongguan Houjie Kaiyan Machinery Equipment Factory, China) at 70°C according to ASTM D 3182. Then, the cure characteristics of the NR compounds were measured by a rotorless curemeter (Shanghai Dejie Equipment Co., Ltd., China) at 150°C×1 h.

Table 1. NR formulation with different antioxidant additions (phr)

Group	1	2	3
Natural Rubber	100	100	100
Zinc oxide	5	5	5
Stearic acid	4	4	4
Sulfur	2.3	2.3	2.3
Accelerator M[a]	0.3	0.3	0.3
Accelerator DM[b]	1.6	1.6	1.6
Antioxidant PAS-Ce	0	1.2	0
Antioxidant 2246	0	0	1.2

[a]M:2-Mercaptobenzothiazole;
[b]DM:2,2′-dibenzothiazoledisulfde.

2.3. Thermal aging experiment

NR samples were placed in a thermal aging chamber at 80°C and aged for 20 days for performance testing. Thermoxic aging NR samples were prepared according to Chinese standard GB3512-1983.

2.4. Hardness performance test

The NR sample was tested for a Shore A Hardness Tester. The center and edge of each sample were tested for at least five times. The hardness test was carried out according to the Chinese standard GB/T531-2008.

2.5. Mechanical testing

NR samples were tested for different aging times using a universal testing machine. Multiple parallel tests were carried out to ensure the accuracy of the experiment. The tensile strength and elongation at break in the specimens were recorded. The tensile speed of the universal testing machine was 500 mm·min^{-1}. The mechanical properties of NR samples were tested according to Chinese GB/T528-2009.

2.6. Fourier infrared test (FTIR-ATR)

FTIR-ATR was used to test the change of functional groups on the surface of three groups on NR samples. The spectrum is obtained in the wavenumber range of 4000∼600 cm^{-1} by using attenuated total reflection technology with a scanning resolution of 4 cm^{-1}.

2.7. Thermogravimetric (TG) test

The TG analysis was carried out on a Thermogravimetric Analyzer (TGA)/Differential Scanning Calorimetry (DSC) calorimeter. Three NR samples weighing 2–5 mg were heated from 30°C to 700°C in an N_2 atmosphere at three heating rates of 10 K/min, 20 K/min, and 30 K/min, respectively. The thermal and oxygen aging behavior of three NR samples was analyzed according to the Kissinger and Flynn-Wall-Ozawa methods [8].

2.8. Quantum mechanical simulation (QM)

The key to quantum mechanics (QM) simulation based on electron nonlocalization was to use an approximate method to carry out the Schrodinger equation for the system. Density Flood Theory (DFT) [9] states that the total energy of the ground state of a multi-particle system was a unique function of electron density. The Kohn–Sham equation was solved to obtain a series of important parameters such as the energy of the ground state and thermodynamic properties of the system. The exchange-correlation potential for the K–S equation was calculated by the PBE generalized function [10]. The inner electron treatment (core treatment) was performed using the DFT Semi-core Pseudopods method, which used a single effective potential instead of the inner core electrons. Relativistic corrections were introduced into the core treatment for heavy elements after atomic number 21. Due to the presence of a single electron in the radical, the spin multiplicity of the system was set to Doublet and optimized using the DND group. To obtain accurate temperature correction values, Frequency was selected in the Properties option. The energy convergence accuracy was set to 1.0e^{-5} Ha to ensure that the constructed molecular structure was fully optimized for convergence.

3. Results and discussions

3.1. Hardness

One of the crucial parameters for measuring the mechanical features of NR was the hardness [11]. In Figure 1, the variations of hardness in NR

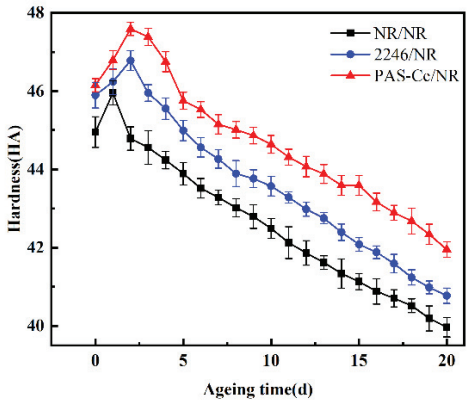


Fig. 1. Changes in hardness of three systems at different aging times at 80°C

specimens treated with distinct anti-aging agents at different aging times under 80°C were given. As seen from Figure 1, the transitions in hardness display a trend of ascent followed by a decline. The primary reason behind such a pattern was related to the absence of a cross-linking reaction at the first stage of aging. Evidently, at high temperatures, the cross-linking reaction increased the cross-linking density and hardness of the NR system. As aging time prolongs, the growing cross-linking density of the NR system engenders a limitation regarding the distortion of the NR molecular chains. Eventually, the system undergoes a reaction that is mainly dominated by molecular chain degradation, resulting in a continuous drop in its cross-linking density [12]. Moreover, the research revealed that the PAS-Ce/NR compound had a lower decline in hardness than the 2246/NR compound, which highlighted the fact that PAS-Ce was more capable and efficient in this regard.

3.2. Mechanical properties analysis

Figures 2(a) and (b) offered a clear insight into the behavior of tensile strength and elongation at break in NR composite systems treated by distinct antioxidants and aged for a considerable amount of time at 80°C. As expected, with the increase in aging duration, the overall tensile strength and elongation at break were seen to decline in both cases. Nevertheless, the mechanistic response to oxidation was comparatively better for the PAS-Ce/NR antioxidant system than the 2246/NR system at equivalent aging intervals. Consequently, it can be safely inferred that the antioxidant PAS-Ce was more successful in safeguarding the system against oxidation damage. In addition, the PAS-Ce/NR composite system emerged as a true winner by demonstrating remarkable mechanical properties even in the face of oxidation-induced aging.

3.3. ATR-FTIR analysis

Figure 3 shows a comprehensive overview of the IR spectra obtained from NR after subjecting it to different timeframes of aging. The plot was segregated into three distinct segments, (a), (b), and (c), depicting the IR spectra of NR, PAS-Ce/NR, and 2246/NR systems, respectively, in the region between 3500–600 cm^{-1}. As discussed in detail in the previous paragraph, the broad peak appearing between 3500 and 3000 cm^{-1} represented the stretching vibration peak of -OH. Intriguingly, the peak intensity at 2848 cm^{-1}, which helped identify the symmetrical stretching vibration of CH_2 on the NR repeat unit, remained unaltered even after aging. This peak's constancy was crucial since it served as a characteristic peak of the NR and its undisturbed state helped validate the accuracy of the analysis. However, as expected, the corresponding stretch vibration peak at 1736 cm^{-1} representing C=O showed a noticeable increase in peak strength with aging time. This phenomenon indicated that various oxidation products such as alcohols, carbonic acids, and peroxides were indeed produced during the thermal-oxidative aging process of NR, leading to the C=O peak's enhancement.

The changes in the intensity of the C=O absorption peak at 1736 cm^{-1} between the three NR systems were highly contrasting after six days of aging, as shown in Figure 3. At the same time, the intensity of the CH_2 bond stretching vibration peak at 2848 cm^{-1} remained unchanged. To quantify the extent of thermal and oxygen aging of NR composites, the ratio of the intensities of the above peaks was used as a reference point as reported

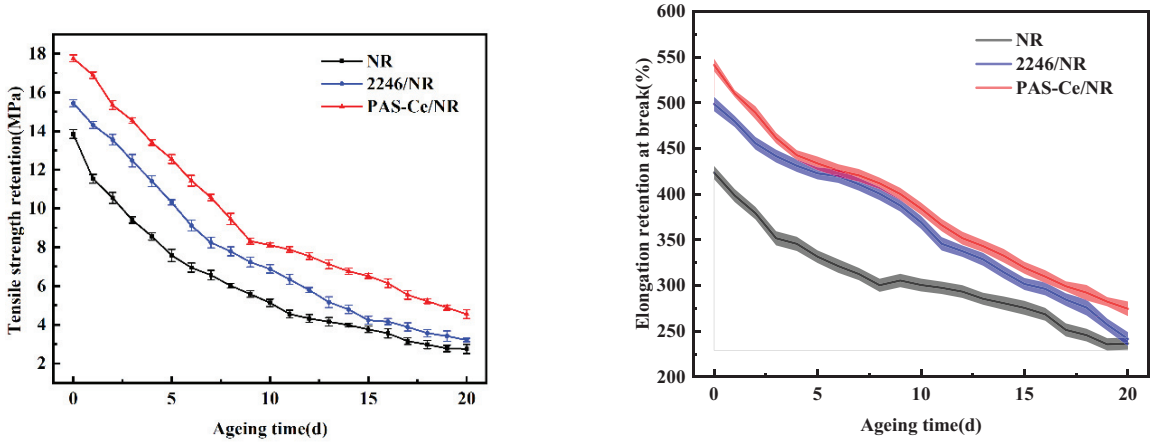


Fig. 2. Tensile strength and elongation retention at the break of three systems with different aging times at 80°C

in [13]. The analysis of the calculated result is presented in Figure 4, showing the different levels of thermal and oxygen aging between the NR composite systems.

An examination of Figure 4 revealed a key observation. Specifically, that the NR material showed a significant increase in absorption intensity after being subjected to the aging process. In contrast, the absorption of the two NR composites with added antioxidants was lower, thus giving the material greater flexibility against the damaging effects of aging. However, it should be noted that the PAS-Ce/NR composites perform very well in terms of aging resistance. This finding was noteworthy as it highlights the effectiveness of antioxidant additives and their unparalleled efficacy in maintaining the properties of NR composites, especially when combined with PAS-Ce.

3.4. Thermal analysis

The use of thermogravimetric analysis (TGA) in the study of polymeric materials, particularly concerning thermal and oxygen aging mechanisms, has proven to be an effective method as described in the literature [14]. To effectively understand the effect of antioxidants on the thermal and oxidative stability of NR, three NR compound systems were analyzed using TG curves to measure their thermal and oxygen-related degradation. The analysis was performed at three different heating rates from room temperature to 700°C at 10°C/min, 20°C/min, and 30°C/min in a nitrogen atmosphere, and the results are shown in Figure 5. As shown in Table 2, a thermal weight loss phase corresponding to the decomposition of NR molecular chains at temperatures between 210°C and 480°C in a nitrogen atmosphere was observed in the TGA curves. It was noteworthy that the characteristic thermal aging and oxygen aging temperatures of NR samples containing PAS-Ce and 2246 antioxidants were significantly higher compared to those of bare vulcanized rubber. This result indicated that the addition of antioxidants to NR composites significantly improved their thermal and oxygen stability, which ultimately improved their overall thermal and oxygen aging properties. In addition, the antioxidant effect of PAS-Ce was found to be superior to that of antioxidant 2246.

3.4.1. Calculation of activation energy of thermal oxygen degradation

To gain a deeper insight into the thermal-oxidative degradation behavior during vulcanization, the Kissinger and Flynn-Wall-Ozawa methods were used for the analysis as detailed in [15]. These methods were used to calculate the activation energy, which was obtained from careful

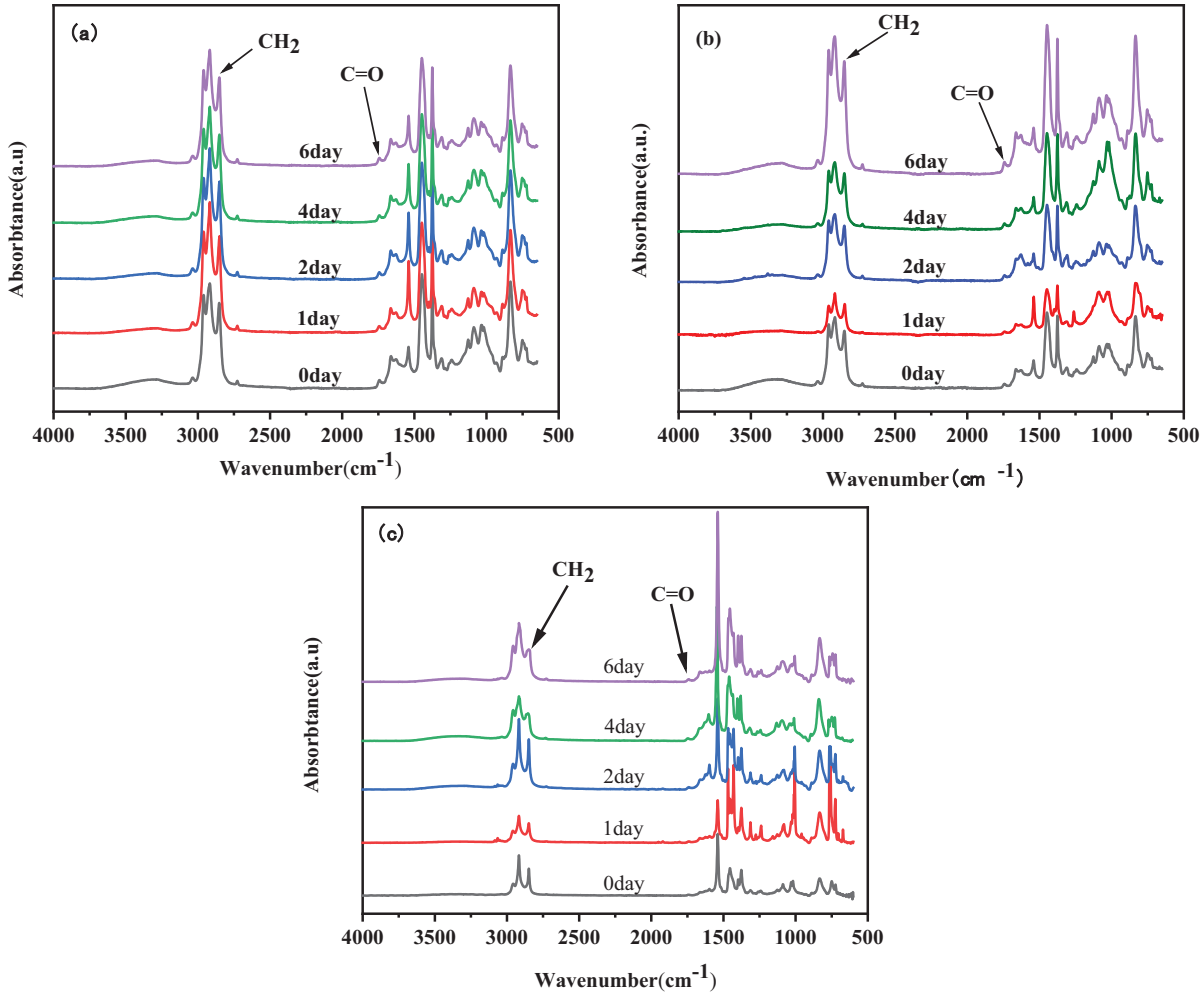


Fig. 3. FTIR of three systems at 80°C before and after 6 days of aging (a) NR (b) PAS-Ce/NR (c) 2246/NR

consideration of the correlation between the maximum peak temperature value and the heating rate, in the course of multiple thermal analyses. By applying these methods, we were able to gain a better understanding of the complex and intricate processes occurring during the thermo-oxidative degradation of vulcanization.

$$\frac{d\alpha}{dt} = Ae^{\left(-\frac{E_a}{RT}\right)}(1-a)^n \tag{1}$$

Where: A is the exponential perfector. E_α is the activation energy in kJ·mol^{-1} and R is the ideal gas constant (8.3145 J/(mol·K)); The following equation for Kissinger is calculated differently for both sides of the above equation [16].

$$\ln\frac{\beta}{T_{max}^2} = \ln\frac{AR}{E_a} - \frac{E_a}{R}\frac{1}{T_{max}} \tag{2}$$

Where: T_{max} is the temperature at the maximum rate of thermal oxygen degradation as determined by the DTG curve. $\ln\beta/T^2_{max}$ was plotted against $1000/T_{max}$ according to the Kissinger equation. The activation energy E_α can be found by finding the slope -E/R.

The relationship between $\ln\beta/T^2_{max}$ and $1000/T_{max}$ determined by the Kissinger method was shown in Figure 6, and the resulting E_α was listed in Table 3.

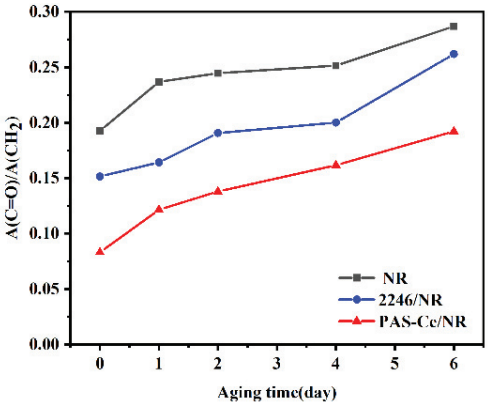


Fig. 4. Absorbance ratio of NR at different times of aging at 80°C for the three systems ($A(C=O)/A(CH_2)$)

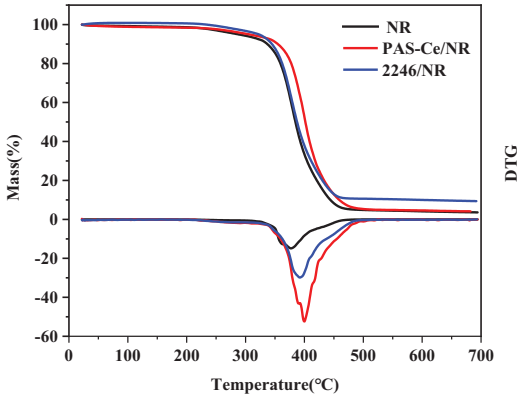


Fig. 5. TG and DTG curves of samples from three NR systems at different warming rates

Table 2. Characteristic temperature of thermal and oxygen aging of different adhesive materials

Category	Blank adhesive material	PAS-Ce/NR	2246/NR
T_0/°C	218	230	236
T_{max}/°C	356	387	345
$T_{0.05}$/°C	287	313	303
T_f/°C	466	480	472

T_0-the temperature at which decomposition begins, T_{max}-the temperature at which decomposition is intense, $T_{0.05}$-the temperature at which it decomposes to 5 percent, T_f-the temperature at the end of decomposition.

Table 3. Activation energy calculated according to the Kissinger method

Category	Blank adhesive material	PAS-Ce/NR	2246/NR
E_a/kJ/mol	149.311	168.615	161.956

The accuracy and reliability of the activation energy of the oxygen thermal decomposition process calculated by Kissinger's method was indisputably confirmed, as evidenced by the fact that the correlation coefficient of all three linear fits was greater than 0.95. Furthermore, a glance at Table 3

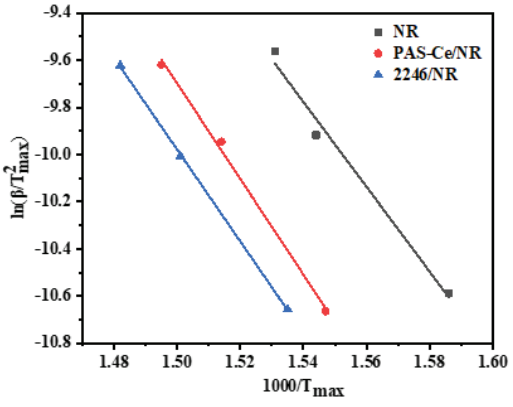


Fig. 6. Plot of $\ln\beta/T^2_{max}$ versus $1000/T_{max}$ determined by the Kissinger method

showed that the addition of the antioxidant PAS-Ce or the antioxidant 2246 significantly increased the thermal oxygen decomposition energy of NR. This, in turn, led to an apparent inhibition of its decomposition. It was noteworthy that the activation energy of thermal oxygen decomposition of the combined PAS-Ce/NR system exceeded the activation energy of the combined 2246/NR system.

According to the report, Kissinger's method was considered a model-free technique for thermal oxygen decomposition processes because it used a different approach without considering the

decomposition model [17]. However, an alternative method, the Flynn-Wall-Ozawa (FWO) method, was introduced to improve the reliability of the activation energy calculated by the Kissinger method, which gave different activation energy values for the thermal decomposition of oxygen. The FWO method derived the activation energy for the thermal decomposition of oxygen by determining the characteristic temperature corresponding to different weight loss rates (β). The activation energy was calculated by comparing β with the logarithm of 1000/T and then with the linear slope obtained by linear fitting. Then, when plotting the activation energy versus weight loss, the range of activation energy values should include the activation energy of the thermal decomposition of oxygen determined by the Kissinger method. It was worth noting that in Figure 7 the correlation coefficient of all fitted lines was greater than 0.96. Thus, the activation energy of the oxygen thermal decomposition process was calculated very reliably for the three NR samples by the FWO method.

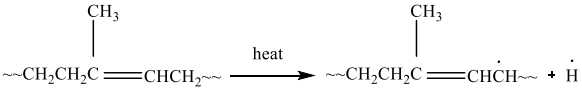
Figure 8 illustrates the correlation between activation energy (E_α) and conversion rate (α) as determined for three NR composite systems by the FWO method. Each curve had an endpoint corresponding to the initial stage of NR backbone failure. Then, an autocatalytic process took place, which led to a decrease in the value of E_α [18]. Interestingly, the PAS-Ce/NR composite system requires significantly higher E_α values for thermotoxic degradation than the 2246/NR system. In addition, three curves ranging from 10% to 60% were integrated to obtain the average E_α range, and then the area values were divided from 65% to 100%. The resulting values are presented in Table 4. It was worth noting that the E_α values were different for different NR composite systems. The PAS-Ce/NR composite system showed a rapid increase in E_α followed by minimal fluctuations, while the 2246/NR system was characterized by a small but relatively constant increase in E_a.

The corresponding E_α values calculated by the Kissinger method fall within the range calculated by the FWO method, so the results were practically reliable and reflect the actual kinetic information.

3.5. Analysis of quantum mechanical simulation results

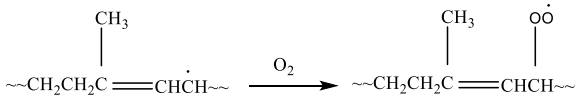
3.5.1. Aging mechanism of NR

As a widespread material in various industries, rubber was often exposed to heat and oxygen in the air. Heat stimulated oxidation and oxygen caused thermal degradation. Therefore, thermal-oxidative aging of rubber was the most common and important way of rubber aging. Thermal oxidative aging of rubber tended to lead to autocatalytic oxidation. In particular, the entire reaction process associated with the thermal oxidative aging of NR occurred through the mechanism of autocatalytic free radical oxidation. This process was divided into three distinct stages [19–21]. (1) Chain initiation: Under the influence of heat and light, the unsaturated double bonds between the molecular structure of the rubber material dissociate, leading to the cleavage and breaking of molecular chains and crosslinks, resulting in the formation of the free radical NR·.



(3)

(2) Chain growth: The reactive R· rapidly combined with oxygen molecules to form the substituent radical ROO·. ROO· continued to react with the rubber molecular chain, forming new radicals R· and the hydroperoxide ROOH, which under certain conditions decomposed to form the radical RO· and the radical HO·. These reactive radicals continued to react with the rubber molecular chain to form alcohols, water, and the R- R-radical. Thus, the R- formed in the previous aging cycle participates in the next cycle. This generates more free radicals and accelerates the thermal oxidative aging process of the rubber. In summary, the thermal oxidative aging process of rubber was characterized by autocatalytic oxidation.



(4)

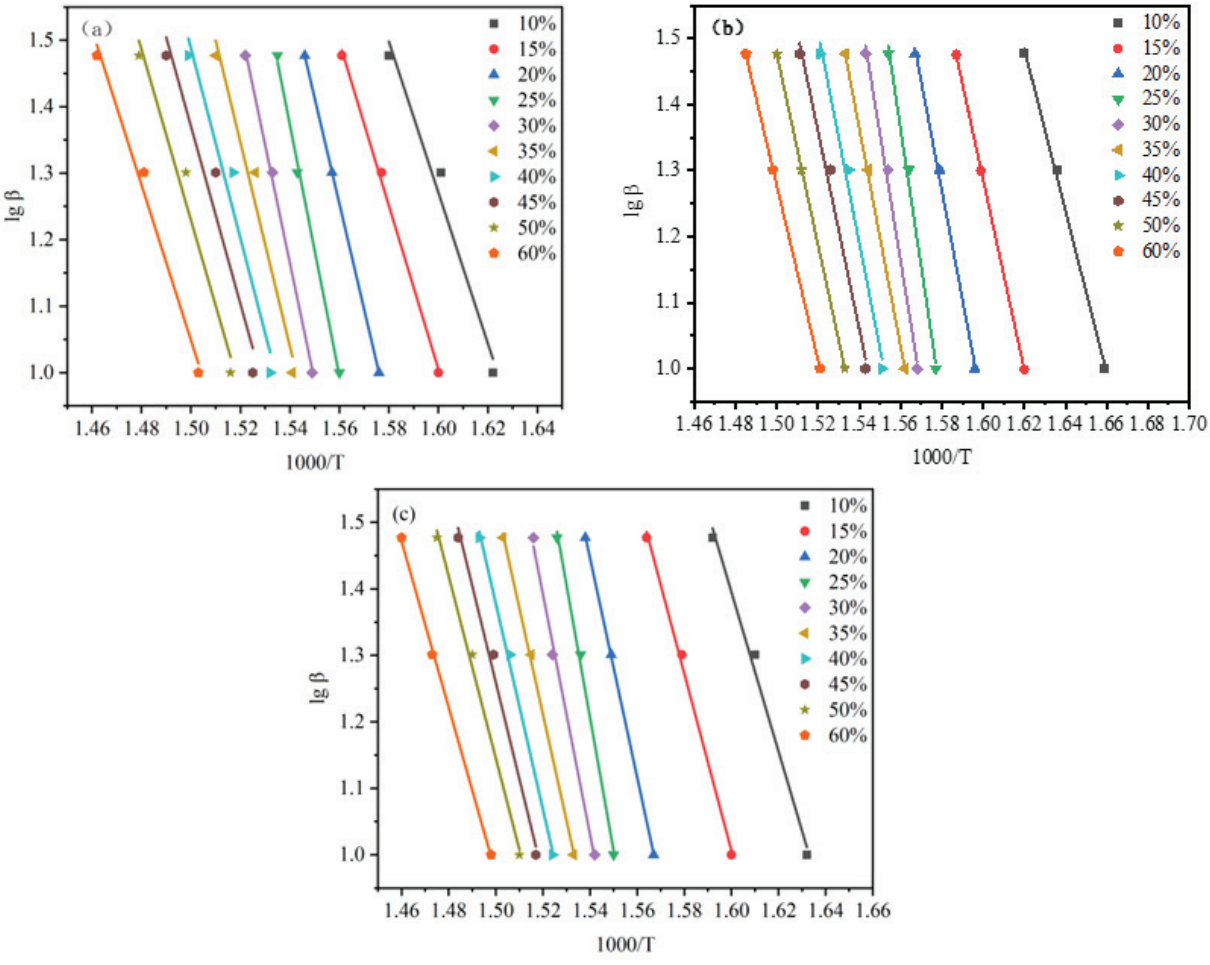
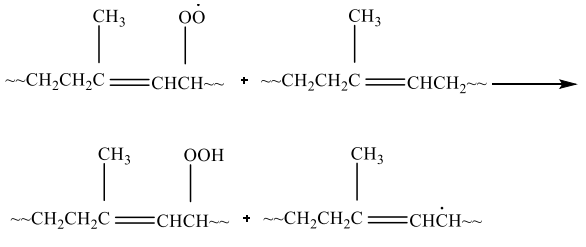


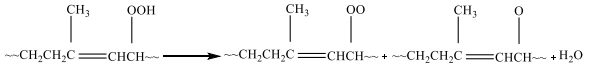
Fig. 7. Relationship between lnβ and 1000/T in three NR complexes determined by FWO at specific weightlessness rates (a) NR (b) PAS-Ce/NR and (c) 2246/NR

Table 4. Activation energy calculated according to the FWO method

Category	Blank adhesive material	PAS-Ce/NR	2246/NR
E_a(kJ·mol^{-1})	94.423∼156.834	102.183∼173.406	99.678∼166.108



(5)



(6)

(3) Chain termination: During the Kautschuk thermal-oxidative aging cycle, free radicals bind to or disproportionate with non-radicals. This completed the chain reaction. As a result, during aging,

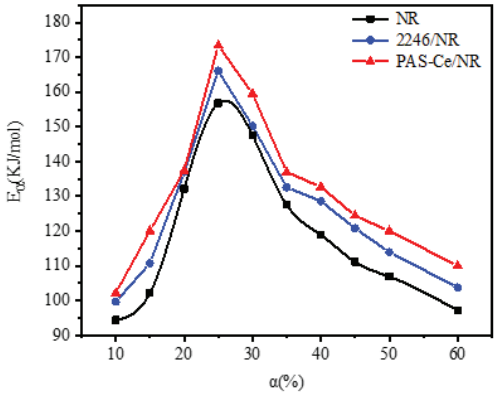
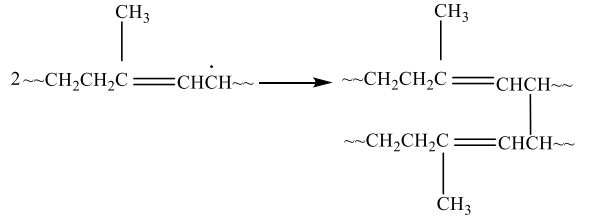
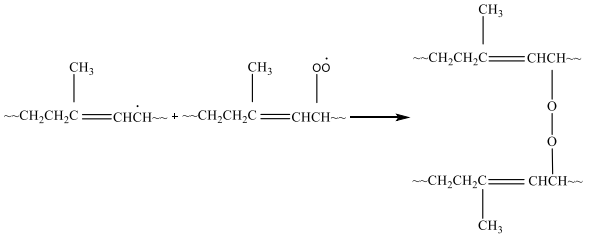


Fig. 8. Relationship between E_α and α in three NR composite systems determined by FWO

some rubber particles became hard and brittle as a result of free radical binding, which increased cross-link density [22], while some rubber particles degraded in molecular chains, reducing cross-link density and becoming sticky and soft [23].



(7)



(8)

Based on the results of the study, it was found that the aging mechanism of NR can be effectively controlled by reducing the concentration of surrogate free radicals in the degradation phase. Interestingly, it was observed that the O-H bond between the PAS-Ce antioxidant and the 2246 antioxidant exhibited significant reactivity and preference towards the agent radical reaction. This directly contributed to reducing the concentration and reaction rate of the substituent radicals in NR, thus effectively preventing its thermal and oxygen aging [24]. Here, it can be firmly concluded that the energy dissipation in O-H bond dissociation reactions between antioxidants can be distinguished by their levels of effectiveness in protecting NR.

3.5.2. Dissociation energy of active hydrogen

The free energies of the C-H bond of the NR molecule, the O-H bond of the PAS-Ce antioxidant, and the dissociation reaction of the 2246 antioxidant were calculated by quantum mechanical (QM) simulations as shown in Figure 9.

After optimizing the desired structural balance, a frequency analysis was performed using the Dmol3 module. This allowed accurate calculations of the zero-point energy at each dissociation point and corrected energy values for the NR configuration. To better understand the effect of temperature on the dissociation reactions, the Gibbs free energy of each dissociation reaction was carefully calculated over the full range of possible operating temperatures of NR, from 200 K to 375 K, at atmospheric pressure. The sum of the electronic energies of the reagent and product radicals calculated for each dissociation reaction at 0 K is given in Table 5. Through these complex calculations and detailed analysis, a deeper understanding of the basic mechanical properties of the dissociation mechanism of NR can be achieved.

A closer reading of the combined data in Table 5 reveals a clear trend: NR has the lowest dissociation energy and the highest activity at position a, which is most susceptible to the damaging effects of oxygen radicals. This important insight suggests that oxidative degradation plays a crucial role in the overall degradation of NR.

For further analysis, Table 6 details the energy corrections of the reactants and products at different temperatures. It is worth noting that no energy correction values for the H- radical at different temperatures are given in this table. These results provide important information for the development of improved methods and techniques aimed at increasing the functionality and durability of NR

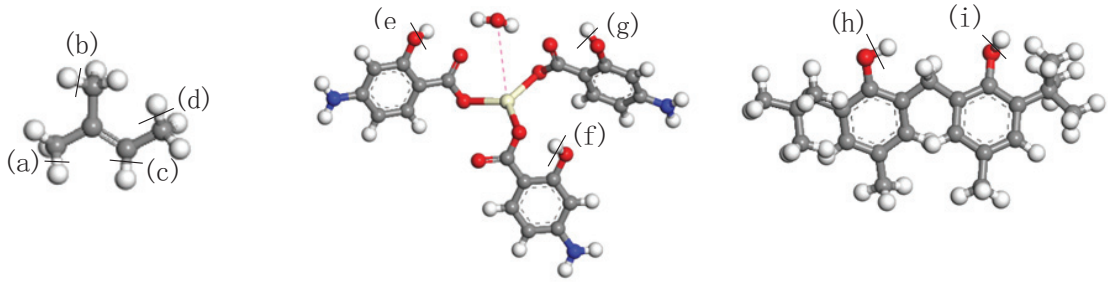


Fig. 9. NR, chemical bond breakage location of antioxidant PAS-Ce and antioxidant 2246 (cyan, gray, blue, white, and red represent lanthanum, carbon, nitrogen, hydrogen, and oxygen, respectively)

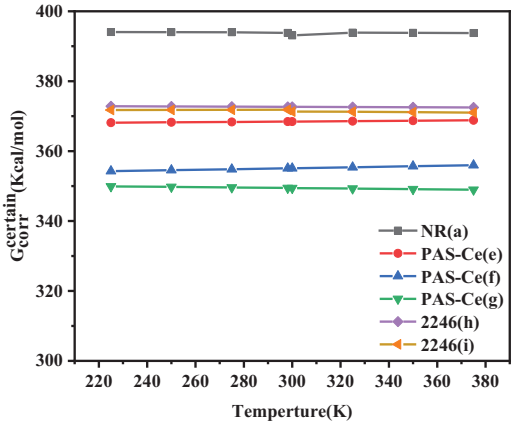


Fig. 10. Free energy of each dissociation reaction at different temperatures

products. Through a nuanced understanding of the complex molecular mechanisms of NR, new solutions can be achieved to optimize its properties.

$$\begin{aligned}\Delta G^{\text{certainK}} = {} & E_{\text{antioxidant}\bullet} \\ & + \Delta G^{(\text{antioxidant}\bullet)\text{certainK}} \\ & + E_{H\bullet} - E_{\text{antioxidant}} \\ & + \Delta G^{(\text{antioxidant})\text{certainK}}\end{aligned} \tag{9}$$

The free energies of each dissociation reaction at different temperatures are listed in Figure 10 according to Equation (9).

After careful analysis of the molecular structure of the two antioxidants, it was found that the dissociation energies of their O-H bonds are lower than those of the C-H bonds in NR. This important discovery led to the understanding that the two antioxidant molecules dissociate readily from NR chains when exposed to thermal-oxidative aging. In addition, both antioxidant PAS-Ce and antioxidant 2246 are effective in dissociating reactive hydrogen radicals with oxygen during aging, thereby terminating the free radical chain reaction initiated in NR during aging.

In addition, it was found that the free energy required to destroy the g-dot was significantly lower than the free energy required to destroy the h-dot. This finding indicates that the antioxidant PAS-Ce was significantly more effective than the antioxidant 2246 in inhibiting the thermal-oxidative aging of NR. This may be due to the electronic structure, atomic number, and coordination ability of the cerium layer. Cerium, which had an empty 4d orbital and a relatively large atomic radius, has a strong coordination ability and was able to trap more radicals growing along the chain, providing better protection for NR.

In essence, the advanced molecular structures of the two antioxidants and their unique properties played an important role in determining the protective effect of NR against thermal-oxidative aging. These discoveries were important for the development of more effective and durable NR products and paved the way for further developments in materials science.

4. Conclusion

In our investigation, we employed a combination of qualitative and quantitative approaches to assess the impact of aging on NR composite materials. Specifically, we conducted a comparative analysis of the anti-aging properties and

Table 5. Total electron energy of each dissociation reaction reactants and radical generators at 0 K

	NR	**NR·(a)**	**NR·(b)**	**NR·(c)**	**NR·(d)**
E/(Ha)	−196.4709459	−195.8011947	−195.8011947	−195.8011947	−195.8011947
	PAS-Ce	PAS-Ce·(e)	PAS-Ce·(f)	PAS-Ce·(g)	2246
E/(Ha)	−1786.38994	−1795.4308478	−1795.4539801	−1795.4249401	−1083.9759531
	2246·(h)	2246·(i)	H·		
E/(Ha)	−1083.40659	−1083.368464	−0.494376		

Table 6. Energy correction values of the reactants and radicals for each dissociation reaction

T(K)	**Energy School is worth $G_{corr}^{certain}$(Kcal/mol)**					
	NR·(a)	**PAS-Ce·(e)**	**PAS-Ce·(f)**	**PAS-Ce·(g)**	**2246·(h)**	**2246·(i)**
200.00	63.045	203.522	204.182	203.446	277.349	276.256
225.00	61.225	198.901	199.726	198.742	273.450	272.447
250.00	59.347	193.999	194.989	193.757	269.301	268.394
275.00	57.412	189.213	190.359	188.894	264.907	264.101
298.15	55.570	188.82	189.978	182.961	260.622	259.913
300.00	55.421	183.37	184.698	177.161	260.270	259.569
325.00	53.376	177.652	179.153	171.099	255.396	254.804
350.00	51.277	171.673	173.349	164.78	250.280	249.807
375.00	49.125	165.437	167.29	158.21	244.947	244.581

mechanisms of PAS-Ce and antioxidant 2246. To achieve this, we utilized a Shaw A hardness tester and a universal testing machine to evaluate the mechanical characteristics of three distinct composite systems (PAS-Ce/NR, 2246/NR, and NR) across various aging durations. Our results revealed that the decrease in hardness within the PAS-Ce/NR system was less pronounced in contrast to the other two systems. Furthermore, the PAS-Ce/NR system demonstrated superior tensile strength and elongation at break when compared to the other systems. During our analysis using infrared spectroscopy, we compared rubber absorption rates at different aging intervals. We measured the ratio of peak values between A(C=O) and A(CH2). Our findings suggested that the PAS-Ce/NR system had the lowest absorption rate, indicating its effectiveness in reducing aging-induced damage. We also conducted two comprehensive thermal analyses and observed that the addition of antioxidants resulted in a significant increase in NR's characteristic thermal aging temperature and oxygen aging temperature compared to that of NR without such additives. Moreover, we discovered that the rare earth antioxidant PAS-Ce considerably increased the activation energy required for the thermal oxidation decomposition of NR, surpassing the effect observed with antioxidant 2246. Moreover, the rare earth element antioxidant PAS-Ce demonstrates robust coordination prowess and multiple coordination numbers, giving it a distinct capacity to neutralize a more significant number of free radicals. This characteristic implies more comprehensive potential applications compared to conventional antioxidants. Furthermore, molecular simulations furnish a theoretical framework for systematically investigating the anti-aging mechanisms of antioxidants in NR compounds, thereby furnishing theoretical insights for selecting appropriate antioxidants in diverse systems.

References

[1] Institute of Synthetic Materials Ageing, Ministry of Chemical Industry, ed. Ageing and anti-ageing of polymeric materials [M]. Beijing: Chemical Industry Press; 1979.

[2] Sulekha PB, Joseph R, Manjooran KB. New oligomer-bound antioxidant in natural rubber/polybutadiene rubber and natural rubber/styrene-butadiene rubber blends[J]. J. Appl. Polym. Sci. 2004;93:437–443, DOI: 10.1002/app.20427.

[3] Fang L, Song YH, Zhu XN, et al. Influence of lanthanum stearate as a co-stabilizer on stabilization sufficiency of calcium/zinc stabilizers to polyvinyl chloride

[J]. Polym. Degrad. Stab. 2009;94(5):845–850, DOI: 10.1016/j.polymdegradstab.2009.01.024.

[4] Xie C, Jia Z, Jia D, et al. The effect of Dy (III) complex with 2-Mercaptobenzimidazole on the thermo-oxidation ageing behavior of natural rubber vulcanizates[J]. Int. J. Polym. Mater. 2010;59(9):663–679, DOI: 10.1080/00914037.2010.483210.

[5] Fang L, Song YH, Zhu XN, et al. Influence of lanthanum stearate as a stabilizer on stabilization efficiency of calcium/zinc stabilizers to polyvinyl ride[J]. Polym. Degrad. Stab. 2009;94(5):845–850, DOI: 10.1016/j.polymdegradstab.2009.01.024.

[6] Zhang YP, Chen J, Guo SH, et al. Application of rare earth type hindered phenolic antioxidants in natural rubber[J]. Rubber Industry. 2013,60(12):738–742, DOI: CNKI:SUN:XJGY.0.2013-12-015.

[7] Chen Z, Zhao X, Guo S. Synthesis of new rare earth antioxidants and research on the protective properties of natural rubber[J]. Chem. Pet. Eng. 2013;26(3):23–29, DOI: CNKI:SUN:SYHX.0.2013-03-005.

[8] Zheng W, Jia Z, Zhang Z, et al. Improvements of lanthanum complex on the thermal-oxidative stability of natural rubber[J]. J. Mater. Sci. 2016;51(19):9043–9056, DOI: 10.1007/s10853-016-0157-4.

[9] Perdew JP. Density-functional approximation for the correlation energy of the inhomogeneous electron gas[J]. Phys. Rev. B Condens. Matter. 1986, DOI: 10.1103/physrevb.33.8822.

[10] Houk KN, Beno BR, Nendel M, et al. Exploration of pericyclic reaction transition structures by quantum mechanical methods: competing concerted and stepwise mechanisms[J]. J. Mol. Struct. 1997;s(398–399):169–179, DOI: 10.1016/s0166-1280(96)04970-6.

[11] Kpulselak J, Sykora R, Hudec I. Sulfur and peroxide curing of Rubber Compounds based on NR and NBR. Part II: Thermo-oxidative Ageing[J]. Kutsch. Gummi Kunstst. 2017.

[12] Xiang KW, Huang GS, Zhong J, et al. Investigation on the thermal oxidative ageing mechanism and lifetime prediction of butyl rubber[J]. Macromol. Res. 2013;21(1):10–16, DOI: 10.1007/s13233-012-0174-3.

[13] Xie C, Jia Z, Jia D, et al. The effect of Dy(III) complex with 2-mercapto benzimidazole on the Thermo-oxidation ageing behavior of natural rubber vulcanizates[J]. Int. J. Polym. Mater. 2010;59(9):663–679, DOI: 10.1080/00914037.2010.483210.

[14] Marinovic-Cincovic M, Jankovic B, Jovanovic V, et al. The kinetic and thermodynamic analyses of the non-isothermal degradation process of acrylonitrile-butadiene and ethylene-propylene-diene rubbers[J]. Compos. B. Eng. 2013;45(1):321–332, DOI: 10.1016/j.compositesb.2012.08.006.

[15] Chen M, Ao N, Zhang B, et al. Comparison and evaluation of the thermo-oxidative stability of medical natural rubber latex products prepared with a sulfur vulcanization system and a peroxide vulcanization system[J]. J. Appl. Polym. Sci. 2010;98(2):591–597, DOI: 10.1002/app.22047.

[16] Chen J, Zhang W, Xiao L, et al. Thermal degradation kinetics of a linked polyurethane acrylate film[J]. J. Test. Eval. 2014;42(2):298–304, DOI: 10.1520/jte20120251.

[17] Lan L, Yu H, Wang S, et al. Thermal degradation behavior of styrene-butadiene-styrene tri-block copolymer/multiwalled carbon nanotubes composites[J]. J. Appl. Polym. Sci. 2010;112(1):524–531, DOI: 10.1002/app.29414.

[18] Nakazono T, Matsumoto A. Mechanical properties and thermal ageing behavior of styrene-butadiene rubbers vulcanized using liquid diene polymers as the plasticizer[J]. J. Appl. Polym. Sci. 2010;118(4):2314–2320, DOI: 10.1002/app.31483.

[19] Xie C, Jia Z, Jia D, et al. The effect of Dy (III) complex with 2-Mercaptobenzimidazole on the thermo-oxidation ageing behavior of natural rubber vulcanizates[J]. Int. J. Polym. Mater. 2010;59(9):663–679, DOI: 10.1080/00914037.2010.483210.

[20] Cunneen JI. Oxidative ageing of natural rubber[J]. Rubber Chem. Technol. 1968;41(1):182–208.

[21] Bevilacqua EM, English ES. The scission step in hevea oxidation[J]. J. Polym. Sci. 1961;49(152):495–505, DOI: 10.1002/pol.1961.1204915229.

[22] Xiang K, Wu S, Huang G, et al. Relaxation behavior and time-temperature superposition (TTS) profiles of thermally aged styrene-butadiene rubber(SBR)[J]. Macromol. Res. 2014;22(8):820–825, DOI: 10.1007/s13233-014-2106-x.

[23] Zheng W, Liu L, Zhao X, et al. Effects of lanthanum complex on the thermos-oxidative ageing of natural rubber[J]. Polym. Degrad. Stab. 2015;120:377–383, DOI: 10.1016/j.polymdegradstab.2015.07.024.

[24] Komethi M, Othman N, Ismail H, Sasidharan S. Comparative study on natural antioxidant as an ageing retardant for natural rubber vulcanizates[J]. J. Appl. Polym. Sci. 2012;124(2):1490–1500, DOI: 10.1002/app.35160.

Received 2023-11-26
Accepted 2024-04-28